

# Density Dependent Spin-Orbit Coupling in Degenerate Quantum Gases

Peng Xu,<sup>1</sup> Tianshu Deng,<sup>1</sup> Wei Zheng,<sup>2,3,\*</sup> and Hui Zhai<sup>1,†</sup>

<sup>1</sup>*Institute for Advanced Study, Tsinghua University, Beijing, 100084, China*

<sup>2</sup>*Hefei National Laboratory for Physical Sciences at the Microscale and Department of Modern Physics, University of Science and Technology of China, Hefei 230026, China*

<sup>3</sup>*CAS Center for Excellence in Quantum Information and Quantum Physics, University of Science and Technology of China, Hefei 230026, China*

(Dated: July 29, 2020)

In this letter we propose a method to realize a kind of spin-orbit coupling in ultracold Bose and Fermi gases whose format and strength depend on density of atoms. Our method combines two-photon Raman transition and periodical modulation of spin-dependent interaction, which give rise to the direct Raman process and the interaction assisted Raman process, and the latter depends on density of atoms. These two processes have opposite effects in term of spin-momentum locking and compete with each other. As the interaction modulation increases, the system undergoes a crossover from the direct Raman process dominated regime to the interaction assisted Raman process dominated regime. For this crossover, we show that for bosons, both the condensate momentum and the chirality of condensate wave function change sign, and for fermions, the Fermi surface distortion is inverted. We highlight that there exists an emergent spatial reflection symmetry in the crossover regime, which can manifest itself universally in both Bose and Fermi gases. Our method paves a way to novel phenomena in a non-abelian gauge field with intrinsic dynamics.

Spin-orbit (SO) coupling is an unambiguous effect in electron gases in quantum materials. For electrons, the SO coupling is essentially a relativistic effect of charged particles, and for a given dispersion in solid, both the form and the strength of the SO coupling are fixed [1, 2]. Although the ultracold atoms are neutral, SO coupling effect can now be simulated for ultracold atoms by utilizing the atom-light interaction [3–5]. In the simplest and most widely used setting, a pair of Raman lasers are applied to ultracold atoms [6–8]. These pair of lasers can flip the spin from down to up, accompanied by a momentum transfer to the right, and simultaneously, can flip the spin from up to down, accompanied by a momentum transfer to the left. In this way, the spin and momentum are locked which realizes the SO coupling effect. Studying SO coupling in ultracold atomic gases can significantly enrich our understanding of this effect. For instance, the effect of SO coupling in a Bose gas [9–28] and its interplay with the BEC-BCS crossover [29–39] are both novel effects revealed by ultracold atomic systems, which have no counterpart in electronic system studied before.

Another unique aspect of SO coupling in ultracold atom systems is that the coupling itself can be made dynamical. That is to say, the dynamics of atoms in the presence of SO coupling can feedback to the coupling form or strength itself. There are two approaches to realize such dynamical SO couplings. One approach is to replace the classical light field with quantum photon field strongly coupled to atoms, for instance, by using cavity field in strong coupling regime [40–42]. Another approach is to make the SO coupling depending on atom field itself, for instance, depending on the density of atoms. Here we will focus on the second approach. The SO coupling can also be viewed as a non-abelian gauge field. Actually, for

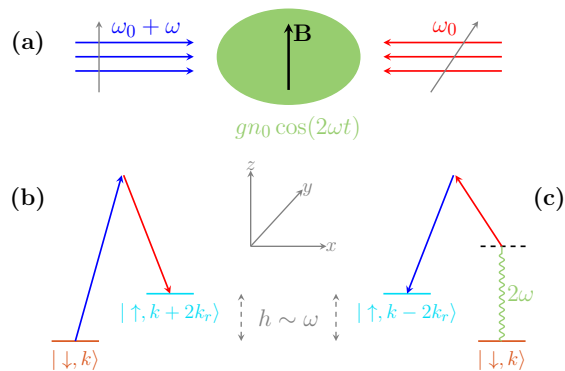


FIG. 1: (a) Schematic of experimental configuration. A pair of Raman lasers with different polarization are applied to a cloud of ultracold atoms. (b) Direct Raman transition regime. (c) Interaction assisted Raman transition regime. For the same spin flip process, the momentum transfer are opposite between (b) and (c).

Abelian gauge field, the  $U(1)$  gauge field, manifested as the phase of hopping in optical lattices, has been made density dependent, either by periodically shaking the optical lattice with a frequency resonant with interaction energy [44], or by periodically driving both optical lattice and interaction [43]. This also enables recent realization of dynamical abelian gauge field with local gauge symmetry [45]. In this letter, we will show that similar method can also be used to realize dynamical SO coupling in both degenerate Bose and Fermi gases. This will be an important step toward realizing dynamical non-abelian gauge field.

*Setting.* First, we consider the conventional configuration where a cloud of ultracold atoms are placed in

two counter propagating Raman beams, as shown in Fig. 1(a). The single particle Hamiltonian is given by

$$\hat{H}_0 = -\frac{\hbar^2 \nabla^2}{2m} + \frac{h}{2} \sigma_z + \hbar \Omega \cos(2k_r x - \omega t) \sigma_x. \quad (1)$$

Here  $h$  is the Zeeman energy between spin-up and spin-down,  $k_r$  is the wave length of the lasers,  $\Omega$  is the strength of the Raman process, and  $\omega$  is the frequency difference between two Raman lasers. Now we apply a unitary rotation  $\hat{U}_1 = e^{-i\omega \sigma_z t/2}$  to Eq. (1), it yields

$$\begin{aligned} \hat{H}_0 = & -\frac{\hbar^2 \nabla^2}{2m} + \delta \sigma_z + \frac{\hbar \Omega}{2} (e^{i2k_r x} \sigma^+ + e^{-i2k_r x} \sigma^-) \\ & + \frac{\hbar \Omega}{2} (e^{-i2k_r x + 2\omega t} \sigma^+ + e^{i2k_r x - 2\omega t} \sigma^-). \end{aligned} \quad (2)$$

where  $\delta = (h - \hbar\omega)/2$ . Usually, considering the situation  $h \sim \hbar\omega$ , we implement the rotating wave approximation to drop the high frequency term, that is the last term in Eq. (2). The retained Raman coupling term is shown in Fig. 1(b), where momentum of an atom increases  $2k_r$  when its spin is flipped from down to up, and decreases  $2k_r$  when it is spin is flipped from up to down. To distinguish with another process discussed below, we refer this process as the direct Raman coupling. With the direct Raman coupling process only, the Hamiltonian can be equivalently written as

$$\hat{H}_0 = \frac{\hbar^2}{2m} (k_x + k_r \sigma_z)^2 + \delta \sigma_z + \frac{\hbar \Omega}{2} \sigma_x. \quad (3)$$

The physical effect of this kind of SO coupling has been discussed extensively in the ultracold atom literatures in the past decade [3–5].

Let us now revisit the term ignored by the rotating wave approximation. This term actually does opposite compared with the direct Raman process. The momentum of an atom decreases  $2k_r$  when its spin is flipped from down to up, and increases  $2k_r$  when it is spin is flipped from up to down, as shown in Fig. 1(c). However, when  $h \sim \hbar\omega$ , the energies between the initial and the final states of this process differs by  $\sim 2\hbar\omega$ . That is also the reason why it can be safely ignored by the rotating wave approximation. However, the situation changes if there exists the periodic driven with frequency  $2\omega$  and coupled to spin degree of freedom, therefore, this  $2\omega$  energy offset can be compensated by this driving [46]. Here we consider periodically modulating spin-dependent interaction with a frequency  $2\omega$ . Such a technique of time periodically modulating interaction is nowadays quite matured in ultracold atom experiments. Thus, the combination of interaction modulation and Raman beam gives rise to another interaction assisted Raman process, as shown in Fig. 1(c). Thus, when interaction modulation is weak, the direct process dominates. And when the interaction modulation becomes strong, the interaction assisted Raman process dominates. In the regime where the interaction assisted dominates, the effective Hamiltonian can

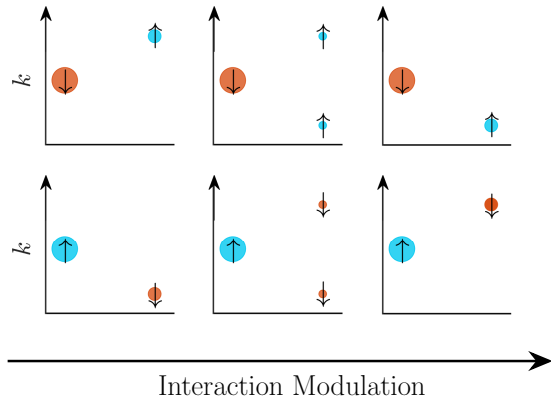


FIG. 2: Schematic of experimental prediction for spin-resolved momentum distribution measured by the time-of-flight with the Stern-Gerlach experiment. The first column dominated by direct Raman coupling regime, the last column dominated by the interaction assisted Raman coupling, and the middle column is the crossover regime where both processes are important. For bosons, the upper row is for  $\delta \gtrsim E_F > 0$  and the lower row is for  $\delta < 0$  and  $|\delta| \gtrsim E_F$ .

be written as

$$\hat{H}_0 = \frac{\hbar^2}{2m} (k_x - k_r \sigma_z)^2 + \delta \sigma_z + \frac{\hbar \tilde{\Omega}}{2} \sigma_x. \quad (4)$$

Note that  $-k_r \sigma_z$  in Eq. (3) is now changed to  $k_r \sigma_z$  in Eq. (4), and  $\tilde{\Omega}/2$  in Eq. (4) is the effective interaction assisted Raman coupling strength, which depends on density.

*Main Results and Experimental Predictions.* Before we introduce the details of our derivations, let us first describe the main results as shown in Fig. 2, which are the experimental predictions as the interaction modulation increases.

For Bose condensation at zero temperature, we consider the situation  $\delta = 0$ . In this case there are two degenerate ground states, where the majority atoms, either spin-up or spin-down, condense at the momentum minimum  $k_{\min}$  around zero. For one state, in the direct Raman coupling regime, majority spin-down atoms are coupled to minority spin-up atoms with positive momentum, and therefore,  $k_{\min}$  is pushed to slightly negative value. If we define a chirality  $\langle k \sigma_z \rangle$  with  $\vec{k} = \vec{k}/|\vec{k}|$ , the chirality is positive. In the interaction assisted Raman coupling regime, in contrast, majority spin-down atoms are coupled to minority spin-up atoms with negative momentum, and therefore,  $k_{\min}$  is pushed to slightly positive value. Then the chirality is negative. In the crossover regime, both direct and interaction assisted Raman processes are equally important, and the minority spin-up atoms appears at both positive and negative momenta. This is schematically shown in the first row of Fig. 2.

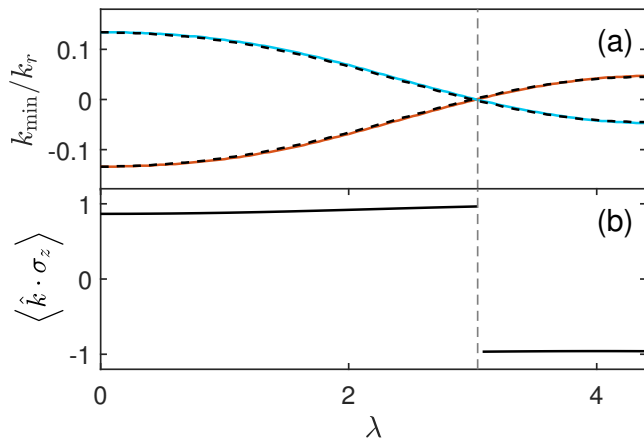


FIG. 3: Bose-Einstein condensate with density-dependent SO coupling. (a) The momentum of energy minima as a function of interaction modulation amplitude  $\lambda = gn_0/(\hbar\omega)$ . Two lines are for two degenerate ground states with  $\sigma_z > 0$  and  $\sigma_z < 0$ , respectively. (b) The chirality  $\langle \hat{k} \cdot \sigma_z \rangle$  of the ground state. The two ground states share the same value of chirality. Here we take  $\delta = 0$  and  $\Omega = 2E_r$ , with  $E_r = \hbar^2 k_r^2 / (2m)$ .

The results from quantitative calculation is shown in Fig. 3, where we show how the momentum minimum and chirality changes when the interaction modulation increases. Especially, one can see that the chirality jumps from positive to negative at the point where  $k_{\min}$  crosses zero. For another degenerate state, the majority spin-up atoms are coupled to minority spin-down atoms with negative momentum in the direct Raman coupling regime, and are coupled to minority spin-down atoms with positive momentum in the interaction assisted Raman coupling regime, as shown in the second row of Fig. 2. Consequently,  $k_{\min}$  changes from positive to negative as interaction modulation increases. The behaviors of the chirality are the same for these two states, as shown in Fig. 3(b).

For degenerate Fermi gas, we consider a simpler situation of one-dimension. When  $\delta \gtrsim E_F > 0$ , the majority fermions are spin-down atoms in absence of SO coupling. The situation is similar as the first row of Fig. 2, with the only difference that atoms populate a Fermi sea instead of occupying the lowest energy state only. In one-dimension, the Fermi surface are simply two points whose momenta are denoted by  $k_F^\pm$  at positive and negative momenta, respectively. Because the Raman process distorts the single particle dispersion and breaks the spatial reflection symmetry, in general  $k_F^+ \neq k_F^-$ . In Fig. 4 we show  $\Delta k_F = k_F^+ + k_F^-$  as a function of interaction modulation strength. It shows that the direct Raman coupling and the interaction assisted Raman coupling distort the fermion dispersion in an opposite way, and therefore,  $\Delta k_F$  changes from negative to positive when interaction modulation increases. If  $\delta < 0$  and  $|\delta| > E_F$ , the majority fermions are spin-up atoms. The situation

behaves as the second row of Fig. 2, and  $\Delta k_F$  changes from negative to positive when interaction modulation increases.

*Method.* We consider modulating the interaction between two spin component as  $g \cos(2\omega t) \hat{n}_\uparrow(\mathbf{r}) \hat{n}_\downarrow(\mathbf{r})$ . For the situation we considered here, to very good approximation,  $\langle \hat{n}_\uparrow(\mathbf{r}) + \hat{n}_\downarrow(\mathbf{r}) \rangle$  is a constant. Therefore, it is convenient to rewrite the interaction Hamiltonian as

$$-\frac{g}{4} \cos(2\omega t) (\hat{n}_\uparrow(\mathbf{r}) - \hat{n}_\downarrow(\mathbf{r}))^2. \quad (5)$$

Here we leave the total density-density interaction for future consideration as it does not enter the Raman processes considered here. We take the mean-field approximation by defining the normalized magnetization as  $M_z(\mathbf{r}) = \langle \hat{n}_\uparrow(\mathbf{r}) - \hat{n}_\downarrow(\mathbf{r}) \rangle / n_0$ , where  $n_0 = N/V$  is the average total density. Then, this mean-field Hamiltonian can be written as

$$\hat{H}_{\text{MF}} = \hat{H}_0 - \frac{g}{2} n_0 M_z(\mathbf{r}) \sigma_z \cos(2\omega t), \quad (6)$$

where  $\hat{H}_0$  is given by Eq. (1). Note that here  $M(\mathbf{r})$  needs to be determined self-consistently.

We employ the Floquet approach to solve this mean-field Hamiltonian. We can define a time evolution operator  $\hat{U}(T) = \int_0^T dt \hat{H}_{\text{MF}}(t)$ . For a given  $M_z(\mathbf{r})$ , we numerically diagonalizing the time evolution operator as  $\hat{U}(T)|\varphi_n\rangle = e^{-i\epsilon_n T/\hbar} |\varphi_n\rangle$ . Here  $\epsilon_n$  is the quasi-energy, which is restricted in the regime  $-\pi\hbar/T < \epsilon_n < \pi\hbar/T$ , and  $|\varphi_n\rangle$  is the corresponding wave function. For bosons, we consider that all atoms are condensed into the state with the lowest quasi-energy. For fermions, we consider that all atoms fill a Fermi sea. Then, we compute  $M_z(\mathbf{r})$  either under this condensation wave function or under the Fermi sea wave function, for bosons or fermions, respectively. We iteratively solve the Floquet Hamiltonian until a self-consistency is reached. Both Fig. 3 and Fig. 4 are obtained by this numerical method, as shown by the solid lines.

To see the physics more clearly, another way is to obtain the Floquet effective Hamiltonian. Here we apply a unitary rotation  $\hat{U}_2$  to the Hamiltonian (6), and

$$\hat{U}_2 = e^{\frac{i}{\hbar} \int_0^t dt' [\frac{\hbar\omega}{2} \sigma_z - \frac{g}{2} n_0 M_z \sigma_z \cos(2\omega t')]}, \quad (7)$$

the Hamiltonian after rotation becomes

$$\hat{H}(t) = -\frac{\hbar^2 \nabla^2}{2m} + \delta \sigma_z + \hbar \Omega \cos(2k_r x - \omega t) \times \begin{pmatrix} 0 & e^{i[\omega t - \frac{\lambda M_z}{2} \sin(2\omega t)]} \\ \text{h.c.} & 0 \end{pmatrix} \quad (8)$$

where  $\lambda = gn_0/(\hbar\omega)$ . Here we have assumed that  $M_z$  is a spatial independent constant, which has been well justified by the numerical method described above. By

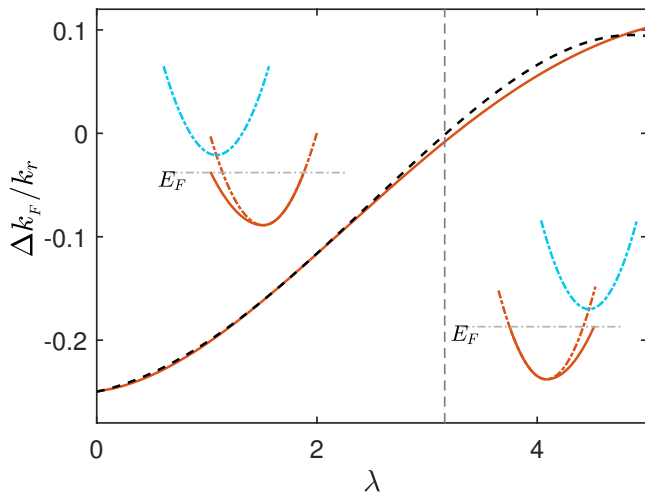


FIG. 4: One-dimensional degenerate Fermi gas with density-dependent SO coupling.  $\Delta k_F = k_F^+ + k_F^-$ , where  $k_F^\pm$  is the Fermi points at positive and negative momenta.  $\Delta k_F$  is plotted as a function of interaction modulation amplitude  $\lambda = gn_0/(\hbar\omega)$ . The inset schematically shows the distortion of fermion dispersion in the direct Raman coupling regime (left) and the density assisted Raman coupling regime (right). Here we set  $\delta = 6E_r$  and  $\Omega = 2E_r$ .

only keeping the zeroth-order of Eq. (8), we obtain a time-independent effective Hamiltonian as

$$\hat{H}_{\text{eff}} = -\frac{\hbar^2 \nabla^2}{2m} + \delta\sigma_z + \frac{\hbar\Omega}{2} \times \begin{pmatrix} 0 & \mathcal{J}_0\left(\frac{\lambda M_z}{2}\right) e^{i2k_r x} + \mathcal{J}_1\left(\frac{\lambda M_z}{2}\right) e^{-i2k_r x} \\ \text{h.c.} & 0 \end{pmatrix}. \quad (9)$$

Here  $\mathcal{J}_0$  and  $\mathcal{J}_1$  is the zeroth and the first order Bessel functions. The numerical results based on Eq. (9) are shown by the dashed lines in Fig. 3 and Fig. 4, which agree well with the solid lines.

The effective Hamiltonian Eq. (9) is a central result of this work. It represents a faithful representation of the density-dependent SO coupling proposed in this work, and illustrates clearly the competition of two Raman processes. In the presence of both positive and negative momentum transfers, the single particle dispersion in general should develop a band structure. For small interaction modulation, when  $\lambda \rightarrow 0$ ,  $\mathcal{J}_0 \rightarrow 1$  and  $\mathcal{J}_1 \rightarrow 0$ . When we ignore  $\mathcal{J}_1$  term, this effective Hamiltonian recovers Eq. (3) upon a gauge transformation, with  $\Omega$  replaced by  $\Omega\mathcal{J}_0(\lambda M_z/2)$ . As  $\lambda$  increases,  $\mathcal{J}_1$  increases and  $\mathcal{J}_0$  decreases. For large interaction modulation, when  $\mathcal{J}_1$  term dominates, by only keeping the  $\mathcal{J}_1$  term, the effective Hamiltonian recovers Eq. (4), with  $\tilde{\Omega}$  given by  $\Omega\mathcal{J}_1(\lambda M_z/2)$ .

*Emergent  $Z_2$  Symmetry.* The crossover between these two regimes happens at  $\mathcal{J}_0(\lambda M_z/2) \approx \mathcal{J}_1(\lambda M_z/2)$ , and a special point is that  $\mathcal{J}_0(\lambda M_z/2) = \mathcal{J}_1(\lambda M_z/2)$ . As we mentioned above, the presence of SO coupling generally breaks the spatial reflection symmetry. However, this

symmetry is restored when  $\mathcal{J}_0(\lambda M_z/2) = \mathcal{J}_1(\lambda M_z/2)$ . As one can see, spatial reflection  $x \rightarrow -x$ , together with a  $\pi$  spin rotation along  $\hat{z}$ , keep the effective Hamiltonian Eq. (9) invariant.

This emergent  $Z_2$  symmetry in the crossover regime has direct experimental signatures. First, as illustrated in the middle column of Eq. (2), the clouds of minority spin component appears at both positive and negative momenta, which are of equal size. Secondly, in Fig. 3 one can see that when  $\lambda = 3.04$ , the condensation momentum  $k_{\text{min}} = 0$ . Thirdly, in Fig. 4 one can see that when  $\lambda = 3.06$ ,  $\Delta k_F = 0$ . Both are indicated by dashed lines in Fig. 3 and 4. It is remarkable to note that although Fig. 3 and Fig. 4 consider two different systems with different  $\delta$ , different dimensionality and different statistics, these two values of  $\lambda$  agree remarkably with each other, because both are determined by the underlying spatial reflection symmetry. This value is also consistent with the condition  $\mathcal{J}_0(\lambda M_z/2) \approx \mathcal{J}_1(\lambda M_z/2)$ , which gives  $\lambda = 2.87$  by taking  $M_z \approx 1$ . In fact, the self-consistent  $M_z$  is close to but smaller than unity when  $\Omega < 4E_r$ , with  $E_r = \hbar^2 k_r^2/(2m)$ , and the actual value of  $\lambda$  for the emergent  $Z_2$  symmetry is slightly larger than 2.87.

*Outlook.* In the past decade, extensive studies have revealed rich physics of ultracold atoms in the presence of a static SO coupling, whose format and strength are both fixed. This work proposes a realistic proposal to realize a density-dependent SO coupling, as given by Eq. (9). Since density of atoms is a dynamical field, this SO coupling has its intrinsic dynamics. Here, as an important initial step to lay down the basis, we only consider the mean-field theory, but more interesting effects can certainly be found in future studies by including density fluctuations. Novel effects can be found particularly in the regime either when density fluctuations are strong, such as in interacting one-dimensional gases, or when the system is sensitive to density, such as in the crossover regime.

*Acknowledgment.* The project is supported by MOST under Grant No. 2016YFA0301600, Beijing Outstanding Young Scholar Program and NSFC Grant No. 11734010.

\* Electronic address: [zw8796@ustc.edu.cn](mailto:zw8796@ustc.edu.cn)

† Electronic address: [huizhai.physics@gmail.com](mailto:huizhai.physics@gmail.com)

- [1] C. Kittel, *Quantum Theory of Solids*, (John Wiley and Sons Inc., 1963)
- [2] R. Winkler, *Spin-orbit Coupling Effects in Two-Dimensional Electron and Hole Systems*, (Springer-Verlag, Berlin, Heidelberg 2003)
- [3] H. Zhai, Int. J. Mod. Phys. B **26**, 1230001 (2012)
- [4] N. Goldman, G. Juzeliūnas, P. Öhberg, and I. B. Spielman, Rep. Prog. Phys. **77**, 126401 (2014)
- [5] H. Zhai, Rep. Prog. Phys. **78**, 026001 (2015)

- [6] Y. J. Lin, K. Jiménez-García, and I. B. Spielman, *Nature* **471**, 83 (2011)
- [7] P. Wang, Z. Q. Yu, Z. Fu, J. Miao, L. Huang, S. Chai, H. Zhai, and J. Zhang, *Phys. Rev. Lett.* **109**, 095301 (2012)
- [8] L. W. Cheuk, A. T. Sommer, Z. Hadzibabic, T. Yefsah, W. S. Bakr, and M. W. Zwierlein, *Phys. Rev. Lett.* **109**, 095302 (2012)
- [9] T. D. Stanescu, B. Anderson, and V. Galitski, *Phys. Rev. A* **78** 023616 (2008)
- [10] C. Wang, C. Gao, C. M. Jian, and H. Zhai, *Phys. Rev. Lett.* **105**, 160403 (2010)
- [11] C. M. Jian, and H. Zhai, *Phys. Rev. B* **84**, 060508 (2011)
- [12] T.-L. Ho, and S. Zhang, *Phys. Rev. Lett.* **107**, 150403 (2011)
- [13] C. J. Wu, I. Mondragon-Shem, and X. F. Zhou, *Chin. Phys. Lett.* **28**, 097102 (2011)
- [14] Z. F. Xu, R. Lü, and L. You, *Phys. Rev. A* **83**, 053602 (2011)
- [15] S. Sinha, R. Nath, and L. Santos, *Phys. Rev. Lett.* **107**, 270401 (2011)
- [16] J.-Y. Zhang, S.-C. Ji, Z. Chen, L. Zhang, Z.-D. Du, B. Yan, G.-S. Pan, B. Zhao, Y. Deng, H. Zhai, S. Chen, J.-W. Pan, *Phys. Rev. Lett.* **109**, 115301 (2012)
- [17] T. Ozawa, and G. Baym, *Phys. Rev. A* **85**, 013612 (2012)
- [18] T. Ozawa, and G. Baym, *Phys. Rev. A* **85**, 063623 (2012)
- [19] Y. Li, L. P. Pitaevskii, and S. Stringari, *Phys. Rev. Lett.* **108**, 225301 (2012)
- [20] G. L. Martone, Y. Li, L. P. Pitaevskii, and S. Stringari, *Phys. Rev. A* **86**, 063621 (2012)
- [21] L. Zhang, J.-Y. Zhang, S.-C. Ji, Z. Du, H. Zhai, Y. Deng, S. Chen, P. Zhang, and J.-W. Pan, *Phys. Rev. A* **87**, 011601 (2013)
- [22] R. M. Wilson, B. M. Anderson, and C. W. Clark, *Phys. Rev. Lett.* **111**, 185303 (2013)
- [23] S. Gopalakrishnan, I. Martin, and E. A. Demler, *Phys. Rev. Lett.* **111**, 185304 (2013)
- [24] Y. Li, G. I. Martone, L. P. Pitaevskii, and S. Stringari, *Phys. Rev. Lett.* **110**, 235302 (2013)
- [25] Q. Zhou, and X. Cui, *Phys. Rev. Lett.* **110**, 140407 (2013)
- [26] S.-C. Ji, J.-Y. Zhang, L. Zhang, Z.-D. Du, W. Zheng, Y.-J. Deng, H. Zhai, S. Chen, and J.-W. Pan, *Nat. Phys.* **10**, 1038 (2014)
- [27] S.-C. Ji, L. Zhang, X.-T. Xu, Z. Wu, Y. Deng, S. Chen, J.-W. Pan, *Phys. Rev. Lett.* **114**, 105301 (2015)
- [28] Z. Wu, L. Zhang, W. Sun, X.-T. Xu, B.-Z. Wang, S.-C. Ji, Y. Deng, S. Chen, X.-J. Liu, J.-W. Pan, *Science* **354**, 83 (2016)
- [29] J. P. Vyasnakere, S. Zhang, and V. B. Shenoy, *Phys. Rev. B* **84**, 014512 (2011).
- [30] Z. Q. Yu, and H. Zhai, *Phys. Rev. Lett.* **107**, 195305 (2011)
- [31] M. Gong, S. Tewari, and C. Zhang, *Phys. Rev. Lett.* **107**, 195303 (2011).
- [32] H. Hu, L. Jiang, X. J. Liu, and H. Pu, *Phys. Rev. Lett.* **107**, 195304 (2011)
- [33] P. Zhang, L. Zhang, and Y. Deng, *Phys. Rev. A* **86**, 053608 (2012)
- [34] L. Zhang, Y. Deng, and P. Zhang, *Phys. Rev. A* **87**, 053626 (2013)
- [35] V. B. Shenoy, *Phys. Rev. A* **88**, 033609 (2013)
- [36] L. Han, and C. A. R. Sa' de Melo, *Phys. Rev. A* **85**, 011606 (2012)
- [37] K. Seo, L. Han, and C. A. R. Sa' de Melo, *Phys. Rev. Lett.* **109** 105303 (2012)
- [38] Z. Fu, L. Huang, Z. Meng, P. Wang, L. Zhang, S. Zhang, H. Zhai, P. Zhang, and J. Zhang, *Nat. Phys.* **10** 110 (2014)
- [39] L. Huang, Z. Meng, P. Wang, P. Peng, S.-L. g Zhang, L. Chen, D. Li, Q. Zhou, J. Zhang, *Nat. Phys.* **12**, 540 (2016)
- [40] Y. Deng, J. Cheng, H. Jing, and S. Yi, *Phys. Rev. Lett.* **112**, 143007 (2014)
- [41] J.-S. Pan, X.-J. Liu, W. Zhang, W. Yi, and G.-C. Guo, *Phys. Rev. Lett.* **115**, 045303 (2015)
- [42] R. M. Kroeze, Y. Guo, B. L. Lev, *Phys. Rev. Lett.* **123**, 160404 (2019)
- [43] L. W. Clark, B. M. Anderson, L. Feng, A. Gaj, K. Levin, and C. Chin, *Phys. Rev. Lett.* **121**, 030402 (2018)
- [44] F. Görg, K. Sandholzer, J. Minguzzi, R. Desbuquois, M. Messer and T. Esslinger, *Nat. Phys.* **15**, 1161 (2019)
- [45] C. Schweizer, F. Grusdt, M. Berngruber, L. Barbiero, E. Demler, N. Goldman, I. Bloch, and M. Aidelsburger, *Nat. Phys.* **15**, 1168 (2019)
- [46] There exists another situation that this  $2\omega$  frequency term cannot be discarded. That is, there is an interaction energy  $\sim 2\omega$  resonant with the  $2\omega$  driving. This can also result in density dependent gauge field and this situation will be reported elsewhere.